

# Metric Residual Networks for Sample Efficient Goal-Conditioned Reinforcement Learning

Bo Liu<sup>1</sup>, Yihao Feng<sup>2</sup>, Qiang Liu<sup>1</sup>, Peter Stone<sup>1,3</sup>

<sup>1</sup>The University of Texas at Austin

<sup>2</sup>Salesforce Research

<sup>3</sup>Sony AI

{bliu, yihao, lqiang, pstone}@cs.utexas.edu

## Abstract

Goal-conditioned reinforcement learning (GCRL) has a wide range of potential real-world applications, including manipulation and navigation problems in robotics. Especially in such robotics tasks, sample efficiency is of the utmost importance for GCRL since, by default, the agent is only rewarded when it reaches its goal. While several methods have been proposed to improve the sample efficiency of GCRL, one relatively under-studied approach is the design of neural architectures to support sample efficiency. In this work, we introduce a novel neural architecture for GCRL that achieves significantly better sample efficiency than the commonly-used monolithic network architecture. The key insight is that the optimal action-value function must satisfy the triangle inequality in a specific sense. Furthermore, we introduce the metric residual network (MRN) that deliberately decomposes the action-value function into the negated summation of a metric plus a residual asymmetric component. MRN provably approximates any optimal action-value function, thus making it a fitting neural architecture for GCRL. We conduct comprehensive experiments across 12 standard benchmark environments in GCRL. The empirical results demonstrate that MRN uniformly outperforms other state-of-the-art GCRL neural architectures in terms of sample efficiency. The code is available at <https://github.com/Cranial-XIX/metric-residual-network>.

## Introduction

Goal-conditioned reinforcement learning (GCRL) refers to the problem in which an agent learns to solve a set of tasks indicated by different “goals” via trial and error. In contrast to the standard reinforcement learning (RL) setting, in which the per-step reward the agent receives can be an arbitrary fixed scalar function, the reward function in GCRL is usually an indicator function identifying whether the agent has achieved the goal but with a varying goal. As a result, GCRL enables the learning of a whole family of tasks with relatively little human effort toward reward design and thus has many potential real-world applications. For instance, robot manipulation tasks like picking and placing an object in a target location can be viewed as a GCRL problem where the underlying task family is parameterized by the target goal lo-

cation. Similarly, robot navigation can be viewed as a GCRL problem where the goal can be any navigation destination.

Although GCRL has a straightforward reward formulation, it inherits the challenges associated with sparse reward learning: unlike in the *dense* reward setting, the reward signal is only informative when the agent reaches the goal. Therefore, sample efficiency is a major challenge in GCRL, meaning that the agent typically needs a large number of interactions with the environment to make meaningful learning progress. To address this problem, an active line of research focuses on designing novel learning algorithms that efficiently use the data. One popular approach is hindsight experience replay (HER) (Andrychowicz et al. 2017), which relabels the agent’s trajectories as if they were aiming to reach the state that they in fact reached, thus rendering every trajectory an example of a successful goal achievement.

One relatively under-explored direction is the design of better neural architectures for GCRL. For actor-critic-like methods, prior work has proposed decomposing the critic function (a.k.a the action-value function  $Q(s, a, g)$ , see Sec. ) into a bilinear network, e.g., either  $Q(s, a, g) = f(s, a)^\top \phi(g)$  (Schaul et al. 2015) or  $Q(s, a, g) = f(s, a)^\top \phi(s, g)$  (Hong, Yang, and Agrawal 2022), where  $f$  and  $g$  are separate neural modules. The principle behind these designs is to inject useful inductive bias into the architecture. Although empirically found to be effective, it remains unclear why such a decomposition works and whether it can be improved upon.

In this work, we argue that one fundamental inductive bias is that under the sparse reward setting, the negated optimal action-value (e.g.,  $-Q^*(s, a, g)$ ) must satisfy the *triangle inequality* in a specific sense. While there exists prior work on neural architectures that respect the triangle inequality (Pitis et al. 2020), we make the following novel contributions:

- We are the first to show that the discounted  $Q^*(s, a, g)$  in the standard GCRL setting (See Sec. ), when the goal is a deterministic onto mapping from the state, satisfies the triangle inequality.
- Motivated by the first point, we introduce the metric residual network (MRN) that deliberately decomposes the negative action-value function (e.g.,  $-Q$ ) into the sum of a metric and an asymmetric residual component,

which provably approximates *any* quasipseudometric.<sup>1</sup>

- With a comprehensive experiment on 12 standard GCRL benchmark environments, MRN consistently performs better than a range of common prior designs. We hypothesize that MRN’s metric component speeds up learning, and the asymmetric residual component makes the approximation accurate.

## Preliminaries

In this section, we first introduce the formal definition of the GCRL problem. Then we review the off-policy actor-critic algorithm DDPG and the hindsight experience replay (HER) method with goal relabeling for GCRL. DDPG+HER serves as the substrate algorithm within which we compare different neural architecture designs.

### Goal-conditioned Reinforcement Learning

The goal-conditioned reinforcement learning problem can be formulated as a goal-conditioned Markov Decision Process, which is an 8-tuple  $M_{\text{gc}} = (\mathcal{S}, \mathcal{A}, \mathcal{G}, T, R, \gamma, \rho_0, \rho_G)$ . Here,  $\mathcal{S}$ ,  $\mathcal{A}$ , and  $\mathcal{G}$  are the state, action, and goal spaces of the agent.  $T : \mathcal{S} \times \mathcal{A} \rightarrow \mathcal{S}$  is the transition dynamics.  $R : \mathcal{S} \times \mathcal{A} \times \mathcal{G} \rightarrow \mathbb{R}$  is the reward function.  $\gamma$  is the discount factor.  $\rho_0$  and  $\rho_G$  are the initial state and target goal distributions. Concretely, at the start of each episode, an initial state  $s_0 \sim \rho_0$  and a goal  $g \sim \rho_G$  are sampled. The agent starts at  $s_0$ , and at each time step  $t \geq 0$ , it chooses action from a policy  $\pi$ , e.g.,  $a_t \sim \pi(\cdot | s_t)$ . It then receives a reward  $r_{t,g} = R(s_t, a_t, g)$  and transitions to the next state  $s_{t+1} \sim T(\cdot | s_t, a_t)$ . The overall objective of the infinite-horizon GCRL problems is to maximize the following:

$$\max_{\pi} J(\pi) = \mathbb{E}_{\substack{s_0 \sim \rho_0, g \sim \rho_G, \\ (s_t, a_t, r_{t,g}) \sim \pi, T, R}} \left[ \sum_{t=0}^{\infty} \gamma^t r_{t,g} \mid s_0, g \right], \quad (1)$$

where the reward  $r_{t,g}$  is often defined as<sup>2</sup>

$$r_{t,g} = R(s_t, a_t, g) = \begin{cases} 0 & M(s_t, a_t) = g \\ -1 & \text{otherwise} \end{cases}. \quad (2)$$

Here  $M : \mathcal{S} \times \mathcal{A} \rightarrow \mathcal{G}$  is an onto mapping from the product space of the state and action to the goal space. Note that  $M_{\text{gc}}$  does *not* terminate when the goal is reached; the agent receives a reward every time it returns to the goal (or remains there). In practice, usually  $\mathcal{G} \subset \mathcal{S}$ . For example, if the goal is for an autonomous car to reach any given velocity, then  $\mathcal{G}$  would naturally comprise the velocity component of the agent’s full state space  $\mathcal{S}$ . For technical reasons in Sec. , we also include  $a_t$  in deciding whether the goal is reached.<sup>3</sup>

<sup>1</sup> $(d, \mathcal{X})$  defines a quasipseudometric on  $\mathcal{X}$  if 1)  $\forall x \in \mathcal{X}, d(x, x) = 0$  and 2)  $\forall x, y, z \in \mathcal{X}, d(x, y) + d(y, z) \geq d(x, z)$ .

<sup>2</sup>There are two conventional setups: either the agent receives a reward of 1 when reaching the goal and 0 otherwise, or it receives  $-1$  reward until it reaches the goal. In this work, without further specification, we assume the latter setting.

<sup>3</sup>When  $r_{t,g}$  is determined by checking whether  $M(s_t, a_t) = g$ , as opposed to whether  $M(s_{t+1}) = g$ , it is a deterministic function involving no randomness from the transition dynamics  $T$ .

## Off-Policy Actor-Critic

Actor-critic methods like Deep Deterministic Policy Gradient (DDPG) (Lillicrap et al. 2015), Twin Delayed DDPG (TD3) (Fujimoto, Hoof, and Meger 2018) and Soft Actor-Critic (SAC) (Haarnoja et al. 2018) are popular methods for solving GCRL. In this work, we consider DDPG as the underlying RL algorithm, as it is the most commonly used method in prior GCRL research. In DDPG and under the GCRL setting, the critic  $Q(s, a, g)$  evaluates the expected discounted return to reach goal  $g$  at state  $s$  by choosing  $a$ . In particular,  $Q(s, a, g)$  is called the *universal value function approximator* (UVFA) as it extends the normal  $Q(s, a)$  to a subset of goals indicated by  $g$ . Formally, we have

$$Q^{\pi}(s, a, g) = \mathbb{E}_{\substack{(s_t, a_t, r_{t,g}) \\ \sim \pi, T, R}} \left[ \sum_{t=0}^{\infty} \gamma^t r_{t,g} \mid s_0 = s, a_0 = a, g \right]. \quad (3)$$

The critic  $Q$  is then updated by minimizing the temporal-difference (TD) error:

$$L(Q) = \mathbb{E} \left[ \left( r_{t,g} + \gamma Q(s_{t+1}, \pi(s_{t+1}), g) - Q(s_t, a_t, g) \right)^2 \right], \quad (4)$$

where the expectation is taken over  $(s_t, a_t, s_{t+1}, g) \sim \mathcal{D}$ , and  $\mathcal{D}$  is the replay buffer that stores the agent’s previous experience. The actor (*a.k.a* the policy  $\pi$ ) is then updated through the critic. In particular, the policy’s gradient in DDPG is

$$\nabla_{\pi} J(\pi) = \mathbb{E} \left[ \nabla_{a_t} Q(s_t, a_t, g) \Big|_{a_t = \pi(s_t)} \right]. \quad (5)$$

### Hindsight Experience Replay

A popular technique for mitigating the sparse reward problem is hindsight experience replay (HER) (Andrychowicz et al. 2017). Assume the agent collects a trajectory  $\tau = (s_0, a_0, \dots, s_T, a_T)$  using policy  $\pi$  and corresponding initial state  $s_0$  and goal  $g$ . If  $\forall t, M(s_t, a_t) \neq g$ , then the agent receives  $-1$  reward every step and therefore learns nothing from this rollout trajectory. HER relabels the trajectory as if the agent were pursuing the goal  $g \in \{M(s_1, a_1), \dots, M(s_T, a_T)\}$ . In this case, the trajectory can be viewed as a successful example of reaching a different goal. By representing  $Q$  as a UVFA (e.g.,  $Q(s, a, g)$ ), one hopes that learning on these relabeled trajectories can help to generalize  $Q$  to all different goals in the goal space, including those from the original goal distribution  $\rho_G$ . In practice, HER is often combined with an off-policy actor-critic algorithm. Following the original work of HER and prior work in GCRL, we use DDPG+HER as the base GCRL algorithm for policy learning and compare the performance across different neural architectures within the critic.

### Metric Residual Network

One way to design a good neural architecture for UVFA is to base it on theoretically sound inductive biases so that the designed networks naturally inherit these inductive biases. Metric residual network (MRN) is designed based on the observation that the optimal universal action-value function  $Q^*(s, a, g)$  in GCRL must satisfy the triangle inequality in

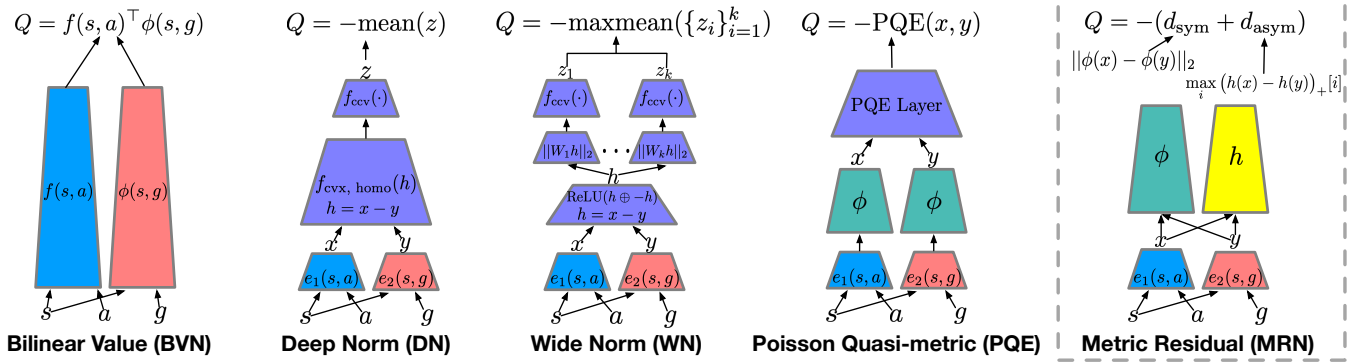


Figure 1: Comparison of different neural architecture designs for decomposing the action value function  $Q(s, a, g)$  in GCRL. For the metric residual network (MRN),  $d_{\text{sym}}(x, y) = \|\phi(x) - \phi(y)\|_2$  and  $d_{\text{asym}}(x, y) = \max_i (h(x) - h(y))_+[i]$ . Note that  $x$  and  $y$  are passed through the *same* networks  $\phi$  and  $h$ . In experiments, all networks are created with approximately the same number of parameters. In particular, the size of  $\phi + e_1$  (or  $h + e_2$ ) in MRN is the same as that of  $f$  (or  $\phi$ ) in BVN.

a specific way. We formally prove this observation is correct in Sec. and introduce a novel network architecture that enforces the triangle inequality in Sec. .

### Triangle Inequality in GCRL

In this section, we start by showing that when  $\mathcal{G} \equiv \mathcal{S} \times \mathcal{A}$ ,  $Q^*(s, a, g)$  satisfies the triangle inequality. Then we extend the result to the general case when  $\mathcal{G} \not\equiv \mathcal{S} \times \mathcal{A}$ .

**When  $\mathcal{G} \equiv \mathcal{S} \times \mathcal{A}$**  Under this setting,  $M$  (in Eq. (2)) becomes the identity mapping. For convenience of notation, let  $\mathcal{X} = \mathcal{S} \times \mathcal{A}$ , i.e.  $x_t = (s_t, a_t)$ . Given a policy  $\pi$ , the universal value function on  $\mathcal{X}$  then becomes

$$Q^\pi(x, x_g) = \mathbb{E}_{\substack{(x_t, r_t) \\ \sim \pi, T, R}} \left[ \sum_{t=0}^{\infty} \gamma^t r_{t,g} \mid x_0 = x, g = x_g \right]. \quad (6)$$

The optimal universal value function is therefore:

$$Q^*(x, x_g) = \max_{\pi} Q^\pi(x, x_g). \quad (7)$$

To build intuition regarding why  $Q^*$  satisfies the triangle inequality, consider any  $x^1, x^2$  and  $x^3$  in  $\mathcal{X}$  (Fig. 2).

Think of  $Q^*(x^1, x^2)$  as consisting of the “cost” of (discounted reward for) reaching  $x^2$  ( $\rightarrow$ ) plus the “cost” of staying at  $x^2$  ( $\dashrightarrow$ ). Decompose  $Q^*(x^2, x^3)$  and  $Q^*(x^1, x^3)$  sim-

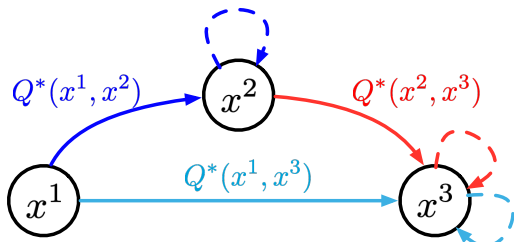


Figure 2: Intuition for triangle inequality in GCRL.

ilarly. Then, by definition of  $Q^*(x^1, x^3)$ , a proof sketch is

$$\begin{aligned} Q^*(x^1, x^3) &= (x^1 \rightarrow x^3) + (x^3 \dashrightarrow x^3) \\ &\geq (x^1 \rightarrow x^2) + (x^2 \rightarrow x^3) + (x^2 \dashrightarrow x^3) \\ &\geq Q^*(x^1, x^2) + Q^*(x^2, x^3). \end{aligned} \quad (8)$$

This statement is formally presented in Thm. 1, and the proof is provided in the Appendix.

**Theorem 1.** Consider the following Goal-conditioned MDP  $M_{gc} = (\mathcal{S}, \mathcal{A}, \mathcal{G}, T, R, \gamma, \rho_0, \rho_g)$  as described in Sec. except that  $\mathcal{G} \equiv \mathcal{S} \times \mathcal{A}$ . Then the optimal universal value function  $Q^*$  defined in Eq. (7) satisfies the triangle inequality:  $\forall x^1, x^2, x^3 \in \mathcal{X}$ ,

$$Q^*(x^1, x^2) + Q^*(x^2, x^3) \leq Q^*(x^1, x^3). \quad (9)$$

Concurrently, Wang and Isola (2022) present a claim similar to Thm. 1, where they show the optimal goal-reaching plan costs in MDPs form a quasipseudometric. The optimal goal-reaching plan cost  $C(x_1, x_2)$  can be viewed as the minimum expected first hitting time from  $x_1$  to  $x_2$ . We emphasize the two differences between Thm. 1 and their statement: **1)** the formulation in Sec. does not assume the agent *terminates* once reaching the goal. Thus the optimal behavior will be *staying* at the goal as long as possible, if necessary, leaving the goal state and returning as quickly as possible. By contrast, the optimal behavior for the first hitting time problem is *hitting* the goal as soon as possible, even if the agent passes the goal, never to return. In practice, sometimes it is possible to change one type of problem to the other by modifying the underlying MDP, but we submit that the problem formulation we consider in Sec. is more relevant and general, as it is the setting used in almost all common GCRL benchmarks and it can always subsume the first hitting time problem by enlarging the state space.<sup>4</sup> **2)** on the other hand,

<sup>4</sup>One can introduce an extra sink state where the agent stays once it reaches the goal to subsume the first hitting time problem into our formulation.

Wang and Isola (2022) state that the optimal goal-reaching plan costs form a quasipseudometric, while we only claim that  $Q^*$  satisfies the triangle inequality. The subtle difference is that within the formulation in Sec. , it is possible that  $Q^*(x, x) \neq 0$  for some  $x \in \mathcal{X}$ .<sup>5</sup> Hence, our formulation is less restrictive.

However, as we will show next, one can still approximate  $Q^*$  well using a quasipseudometric in a larger space. For instance, assume we have a copy of  $x$  denoted  $\hat{x}$  for every  $x \in \mathcal{X}$ . Call the space  $\mathcal{Y} = \mathcal{X} \cup \hat{\mathcal{X}}$ , where  $\hat{\mathcal{X}} = \{\hat{x}\}$ . Then consider the following function  $\hat{Q} : \mathcal{Y} \times \mathcal{Y} \rightarrow \mathbb{R}_{\leq 0}$ :

$$\hat{Q}^*(a, b) = \begin{cases} 0 & a = b \\ Q^*(a, a) & b = \hat{a}, a \in \mathcal{X} \\ Q^*(a, b) & a \neq b, a, b \in \mathcal{X} \\ -\infty & \text{otherwise.} \end{cases} \quad (10)$$

It is easy to check that **1**)  $-\hat{Q}^*$  is a quasipseudometric on  $\mathcal{Y}$ , **2**)  $\forall x, y \in \mathcal{X}$ ,  $\hat{Q}^*(x, e(y)) = Q^*(x, y)$ , where  $e(y) = y$  if  $x \neq y$  and  $e(y) = \hat{y}$  if  $x = y$ . Therefore, though  $Q^*$  only needs to satisfy triangle inequality on  $\mathcal{X}$ , by mapping  $y$  to  $e(y)$ ,  $\hat{Q}^*$ , a negated quasipseudometric, represents  $Q^*$ .

**When  $\mathcal{G} \not\cong \mathcal{S} \times \mathcal{A}$**  Under this setting,  $M$  (in Eq. (2)) is an onto mapping, meaning that there might exist multiple  $(s, a)$  pairs mapping to the same goal. If the underlying transition dynamics  $T$  is *deterministic*, one observes that

$$Q^*(x, g) = \sup_{x': M(x')=g} Q^*(x, x'). \quad (11)$$

Therefore, when the sup is attainable, denote  $x_g =_{x': M(x')=g} Q^*(x, x')$  then  $Q^*(x, g) = Q^*(x, x_g)$ . The proof and more discussion are in the Appendix. As a result, we can view  $Q^*(s, a, g)$  as a specific “distance”<sup>6</sup> between  $x = (s, a)$  and  $x_g$ , which leads to our design of the neural architecture in the following section.

## Network Design

In this section, we first present a novel construction for quasipseudometrics and prove that it universally approximates any quasipseudometric. Then we present a novel neural architecture for GCRL based on this construction and show in a toy example why such design improves generalization and therefore sample efficiency. Lastly, we provide a unified view of existing architecture designs for GCRL.

**A Novel Construction for Quasipseudometrics** From the observations in Eq. (10)-(11), we know  $Q^*(s, a, g) = Q^*(x, x_g)$ , where the latter can be represented by a negated quasipseudometric  $\hat{Q}^*$ . Therefore, we first present a novel construction for quasipseudometrics in Prop. 2.

**Proposition 2.** Assume  $x, y \in \mathcal{X}$ , define

$$d(x, y) = d_{\text{sym}}(x, y) + \underbrace{\max_{i \in [K]} (h_i(x) - h_i(y))}_{{d_{\text{asym}}(x, y)}}, \quad (12)$$

<sup>5</sup>For instance, there are no actions that ensure the agent can stay at  $x$  forever, i.e., it needs to come out and return to  $x$  repeatedly.

<sup>6</sup>Quotation marks are used to indicate that  $Q^*$  might not be a true distance function as it is not guaranteed to be symmetric.

where  $(\cdot)_+ = \max(\cdot, 0)$  is the Rectified Linear Unit (ReLU) function,  $h_i : \mathcal{X} \rightarrow \mathbb{R}$ , and  $(\mathcal{X}, d_{\text{sym}})$  is a metric. Then  $d$  ensures the three axioms of quasipseudometrics:

- *Non-negativity:*  $\forall x, y \in \mathcal{X}, d(x, y) \geq 0$ .
- *Identity:*  $\forall x \in \mathcal{X}, d(x, x) = 0$ .
- *Triangle inequality:*

$$\forall x, y, z \in \mathcal{X}, d(x, z) \leq d(x, y) + d(y, z).$$

In practice, we choose  $d_{\text{sym}}(x, y) = \|\phi(x) - \phi(y)\|_2$  where  $\phi$  is an arbitrary neural network. Clearly,  $\forall x, y, d_{\text{sym}}(x, y) = d_{\text{sym}}(y, x)$ , and with the ReLU function,  $d_{\text{asym}}$  is asymmetric, i.e.  $\exists x, y, d_{\text{asym}}(x, y) \neq d_{\text{asym}}(y, x)$ .

The proof is provided in the Appendix. Prop. 2 ensures that any construction of  $d$  in the form of Eq. (12) is a quasipseudometric, but does not guarantee that any quasipseudometric on  $\mathcal{X}$  can be represented in the form of  $d$ . The following theorem confirms that this is indeed the case.

**Theorem 3** (Universal approximation of  $d$ ). Given any continuous function  $\nu : \mathcal{X} \times \mathcal{X} \rightarrow \mathbb{R}$ , where  $(\mathcal{X}, \nu)$  is a quasipseudometric and  $\mathcal{X}$  is compact. Then  $\forall \epsilon > 0$ , with a sufficiently large  $K$ , there exists a quasipseudometric  $d$  in the form of Eq. (12) such that

$$\forall x, y \in \mathcal{X}, |d(x, y) - \nu(x, y)| \leq \epsilon.$$

The proof is provided in the Appendix.

**A Novel Architecture for GCRL** Based on the novel construction of a quasipseudometric in Eq. (12), we introduce the metric residual network (MRN) for GCRL problems, which consists of two parts:

- *Projection:* with two encoders  $e_1 : \mathcal{S} \times \mathcal{A} \rightarrow \mathcal{Z}$  and  $e_2 : \mathcal{S} \times \mathcal{G} \rightarrow \mathcal{Z}$ , we project  $(s, a, g)$  to two latent vectors:

$$h_{sa} = e_1(s, a), \quad h_{sg} = e_2(s, g).$$

- *Enforcing triangle inequality:* with  $d_{\text{sym}}$  and  $d_{\text{asym}}$  defined in Eq. (12), represent:

$$Q(s, a, g) = - \left( d_{\text{sym}}(h_{sa}, h_{sg}) + d_{\text{asym}}(h_{sa}, h_{sg}) \right).$$

In the projection step, one can view  $e_1(s, a)$  and  $e_2(s, g)$  as summarizing the sufficient statistics of  $x$  and  $x_g$  and projecting them to the same latent space  $\mathcal{Z}$ . In theory,  $x_g$  should be a function of  $s, a, g$ . The reason why we omit  $a$  from the inputs to  $e_2$  is that otherwise  $e_2$  has all the information needed to predict  $Q^*$  directly, which makes the decomposition to  $x$  and  $x_g$  meaningless and thus slows down training (See the ablation study in Sec. for empirical evidence). After the projection step,  $d_{\text{sym}}$  and  $d_{\text{asym}}$  act as the inductive bias that constrains the learning on the latent space  $\mathcal{Z}$ . **The core intuition** behind decomposing  $d$  into  $d_{\text{sym}}$  and  $d_{\text{asym}}$  is that  $d_{\text{sym}}$ , due to its symmetry, *improves sample efficiency*, while  $d_{\text{asym}}$  *ensures the approximation is accurate*.

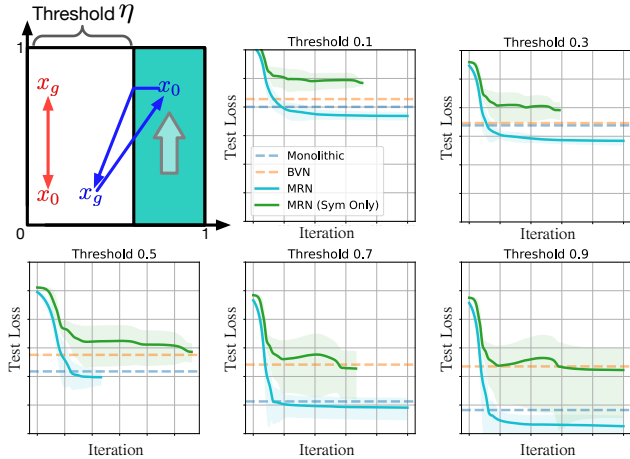


Figure 3: A toy example for illustrating the importance of both the symmetric and asymmetric parts in MRN.

**Toy Example** We provide a toy example in Fig. 3 (top-left) to validate **1)**  $d_{\text{sym}}$  helps improve generalization, and **2)**  $d_{\text{asym}}$  helps improve the modeling accuracy. The environment is a square of size 1. The agent navigates freely in the white region (w/ width  $\eta$ ), and is constrained to move in directions that do not decrease its height in the indigo region. Clearly, the shortest path length  $d^*(x_0, x_g)$  is a quasipseudometric. We then approximate  $d^*$  by  $d_\theta$ . To test  $\theta$ 's generalization ability, we consider supervised learning on 20 data points  $\{(x_0, x_g), d^*(x_0, x_g)\}$ , where  $x_0, x_g \in [0, 1]^2$  are sampled uniformly at random.<sup>7</sup> In the rest of Fig. 3, we plot the *generalization* error over training iteration for different thresholds  $\eta$ , when  $\theta$  is either MRN or MRN with only  $d_{\text{sym}}$ .<sup>8</sup> For reference, we also plot the best generalization error of the bilinear value network (BVN) (Hong, Yang, and Agrawal 2022) and monolithic network, as other designs including the deep/wide norms (Pitis et al. 2020) fail to work in this toy example. The generalization error is evaluated on 10000 randomly sampled  $(x_0, x_g)$  pairs different from the training data. Each curve is plotted to the iteration that reaches the lowest generalization error. From the figures, we observe that **1)** as threshold  $\eta$  increases, the generalization error of MRN decreases because  $d^*$  becomes more symmetric; and **2)** the symmetric part alone (green) does not approximate  $d^*$  well as  $d^*$  is asymmetric.

To summarize, the design of MRN not only incorporates the inductive bias that  $Q^*$  must satisfy the triangle inequality but also ensures it can universally approximate any  $Q^*$  with good generalization ability by having both the  $d_{\text{sym}}$  and  $d_{\text{asym}}$  parts. For the convenience of understanding and implementation of MRN, we provide the forward pass of MRN in PyTorch-like pseudocode in Alg. 1 in the Appendix.

**A Unified View of Existing GCRL Architectures** Recent work proposed Deep Norm (DN) and Wide Norm

<sup>7</sup>For simplicity,  $d_\theta$  directly regresses to  $d^*$  without doing RL, hence no actions are involved.

<sup>8</sup>MRN with only  $d_{\text{sym}}$  is expanded to match the size of MRN.

(WN) (Pitis et al. 2020), which also satisfy the triangle inequality by design. However, both DN and WN are norm-based networks, i.e., they are restricted to only approximate norm-induced quasi-metrics. On the other hand, the conventional monolithic multi-layer perceptron (MLP) modeling  $Q(s, a, g)$ , and the recently proposed bilinear value network (BVN) (Hong, Yang, and Agrawal 2022) both inherit the universal approximation guarantee from general neural networks, but they do not enforce the triangle inequality, thus making them less computationally efficient to learn. The Poisson Quasi-metric Embedding (PQE) (Wang and Isola 2022) enjoys the same theoretical guarantee as MRN. However, MRN is simpler in structure and empirically performs better than PQE (See Sec. Experiment).

## Related Work

A brief summary of previous attempts to approximate the action-value function is presented in the following.

Early work considered linear functions as parametric models for value function approximation (Sutton and Barto 2018; Littman and Sutton 2001; Singh et al. 2003). Successor featured (Dayan 1993; Kulkarni et al. 2016; Borsa et al. 2018) is another line of work that assumes the reward is a linear function of the state-action features (e.g.  $R(s, a) = w^\top \phi(s, a)$ ). Therefore,  $Q(s, a) = w^\top \psi(s, a)$  where  $\psi(s, a)$  is the discounted expected state-action feature occupancy. While linear functions are well-studied and relatively supportive of proving convergence properties, they can be too restrictive to approximate the value function in practical problems. Laplacian reinforcement learning (Mahadevan and Maggioni 2005) instead represents the value function based on a set of Fourier series. All of the above work discussed so far learns the action-value function in a single-task setting, without considering the more general goal-conditioned setting.

More recently, researchers have considered how to decompose the *universal value function approximator*  $Q(s, a, c)$  where  $c$  can be any context variable (e.g. a goal  $g$  or a specific task  $k$ ). In particular, for GCRL, Schaul et al. (2015) consider the low-rank bilinear decomposition, i.e.  $Q(s, a, g) = f(s, a)^\top \phi(g)$ . The motivation behind bilinear value networks is that decomposing  $Q(s, a, g) = f(s, a)^\top \phi(s, g)$  may result in better learning efficiency compared to the low-rank bilinear decomposition (Hong, Yang, and Agrawal 2022). Besides the above approaches designed specifically for GCRL, Pitis et al. (2020) proposed the Deep Norm (DN) and Wide Norm (WN) families of neural networks that respect the triangle inequality. Note that norms always respect the triangle inequality, and DN is a network that essentially computes some norm between two points  $x$  and  $y$ . However, to relax one additional assumption of norms called homogeneity, i.e.  $D(c \cdot (x - y)) = cD(x - y)$ , DN adds a concave function on top of the convex neural network. But even with this relaxation, DN still cannot represent all functions that respect the triangle inequality as the input to DN is restricted to be  $x - y$ . WN is essentially any linear or maxout combination of DN networks. While DN and WN can approximate a rich family of functions, they are still restricted to norm-induced functions. Concurrently,



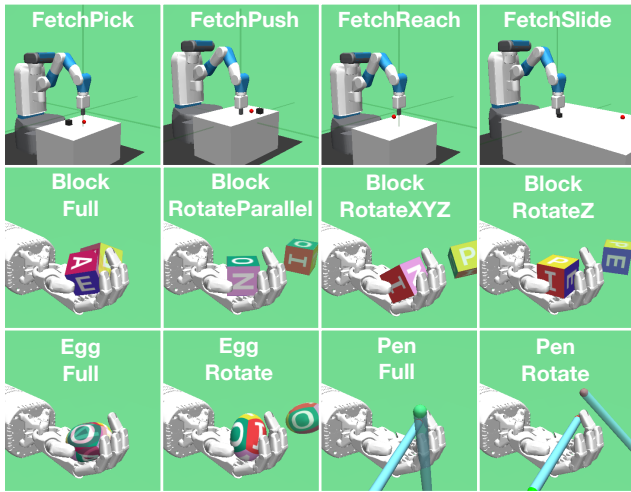


Figure 4: The 12 GCRL environments.

Poisson Quasi-metric Embedding (PQE) has been proposed, which approximates any quasipseudometric from a distribution perspective (Wang and Isola 2022). PQE improves upon DN/WN as it can universally approximate any quasipseudometric function. However, as explained in detail in Sec. , when applied to RL problems, PQE considers the more restrictive first hitting-time problem, while we consider the general GCRL setting. By explicitly decomposing the network into a metric part plus an asymmetric residual part, MRN can learn more efficiently. In addition, the design of DN, WN, and PQE are relatively complicated and may require careful hyperparameter tuning in practice. By contrast, MRN is much simpler and involves no hyperparameters.

## Experimental Results

Experiments are designed to validate two hypotheses: 1) MRN achieves better sample efficiency compared to the baseline methods (Sec. ), and 2)  $d_{\text{sym}}$  and  $d_{\text{asym}}$  are both important in the design of MRN. We start by introducing the benchmarks and baseline methods and provide the experiment details. Then we provide the results and analysis indicating that they confirm our hypotheses.

**Benchmarks** We use the standard GCRL benchmarks (Plappert et al. 2018) including all manipulation tasks on the *Fetch* robot and *Shadow-hand* (See Fig. 4).

**Baselines** We compare MRN with a comprehensive list of existing UVFA architectures as illustrated in Fig. 1:

- *Monolithic*:  $Q(s, a, g)$  is an unconstrained neural network that directly maps  $(s, a, g)$  to the value.
- *Bilinear Value Network* (BVN) (Hong, Yang, and Agrawal 2022):  $Q(s, a, g) = f(s, a)^\top \phi(s, g)$ .
- *Deep/Wide Norms* (DN/WN) (Pitis et al. 2020). DN/WN are networks that represent norm-induced metrics. The original DN/WN operates on the space where the metric is defined. To adapt them to the GCRL setting, we apply DN/WN to  $h_{sa}$  and  $h_{sg}$  with the same encoders as MRN.

- *Poisson Quasi-metric Embedding* (PQE) (Wang and Isola 2022). PQE represents quasi-metrics from a distribution perspective.

**Algorithm and architecture** We use deep deterministic policy gradient (DDPG) (Lillicrap et al. 2015) with hindsight experience replay (HER) (Andrychowicz et al. 2017) as the base GCRL algorithm, within which we test all different architectures. Specifically, we only change the critic architecture  $Q(s, a, g)$ . We constrain different networks to have the same number of parameters to equalize learning capacity. The monolithic network is a three-hidden-layer multi-layer perceptron (MLP) with 256 neurons per layer with ReLU activation (e.g. `[linear-relu]×3 + linear`). BVN has two separate networks  $f$  and  $\phi$ , each of which is a three-layer MLP with 176 neurons per layer. For all other networks, we first define two encoders  $e_1$  and  $e_2$  (e.g. `[linear-relu]×2`). DN, WN, and PQE have method-specific modules on top of the two encoders, which follow the corresponding published implementation. For MRN, both the metric part  $d_{\text{sym}}$  and the residual asymmetric part  $d_{\text{asym}}$  are a single hidden layer neural network with 176 neurons (e.g., `linear-relu-linear`). The actor network is the same as the monolithic critic network except that the output layer projects to the action space.

**Evaluation** For each architecture and each environment, we evaluate with 5 independent seeds  $\{100, 200, 300, 400, 500\}$ . The agent is trained on 1000 episodes of data each epoch. After each training epoch, we evaluate the agent by recording its average performance (success rate) over 100 independent rollouts with randomly sampled goals. We plot the average success rate over learning epochs, averaged over the 5 seeds, along with its standard deviation (shaded region).

### MRN Achieves Better Sample Efficiency

The GCRL experiment results using different state-of-the-art neural architectures as the critic is presented in Fig. 5. Note that within BVN, DN, WN, and PQE, no single method performs uniformly better than all other methods across all environments. By contrast, MRN performs comparably to or better than all baseline methods in all environments.

### On Importance of Both $d_{\text{sym}}$ and $d_{\text{asym}}$

To validate the necessity of decomposing MRN into  $d_{\text{sym}}$  and  $d_{\text{asym}}$ , we conduct an ablation study that experiments with each part alone. To match the learning capacity, we enlarge the  $d_{\text{sym}}$ -only and  $d_{\text{asym}}$ -only networks to have 300 neurons per layer. The results are depicted in Fig. 6. From the figure, we can see that the  $d_{\text{sym}}$ -only network converges faster than the  $d_{\text{asym}}$ -only network. However, neither alone achieves the best sample efficiency or final performance. This result further confirms the necessity of combining both parts. To exclude the case that MRN outperforms the ablated networks due to the learning rate, we double the learning rate for the ablated methods, and the result is in the Appendix. Recall from Sec. Metric Residual Network (Fig. 1), whereas in theory,  $x_g$  is a function of  $s, a, g$ , in practice, we only provide  $s, g$  as inputs for the sake of efficiency. To validate this

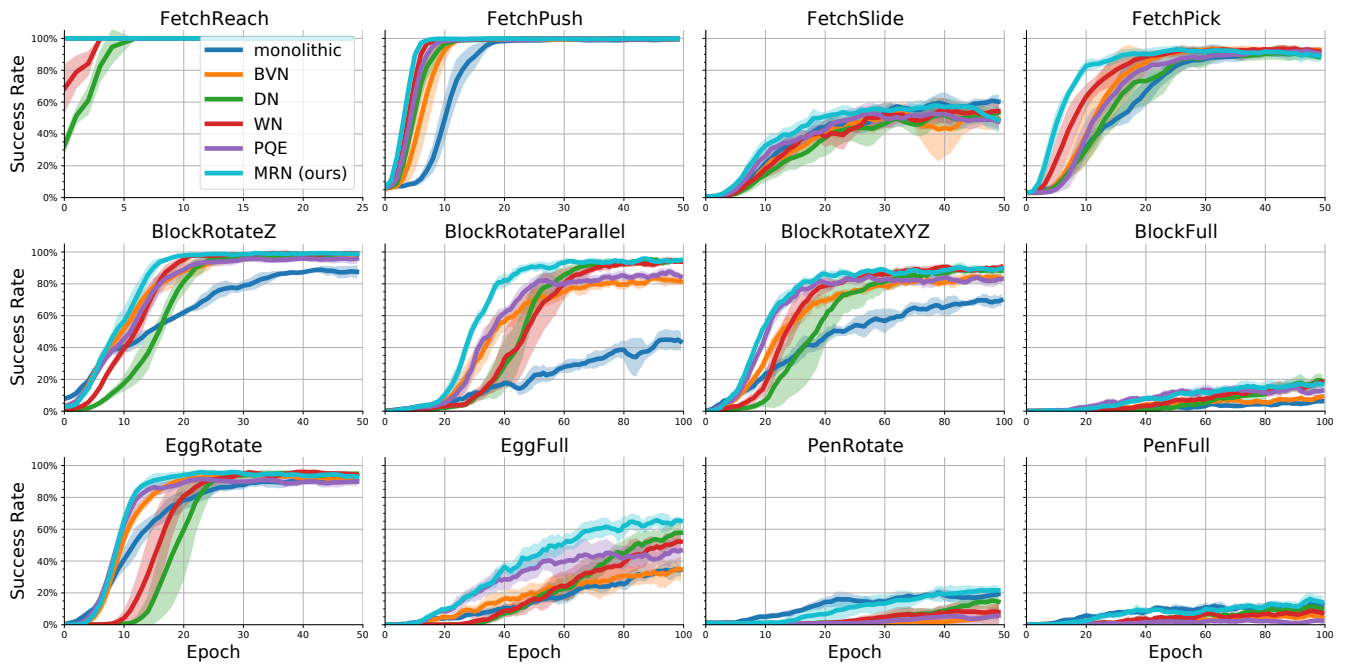


Figure 5: Success rate over training epochs for MRN (ours), the monolithic network, BVN (Hong, Yang, and Agrawal 2022), DN and WN (Pitis et al. 2020), and PQE (Wang and Isola 2022), on 12 GCRL environments from (Plappert et al. 2018).

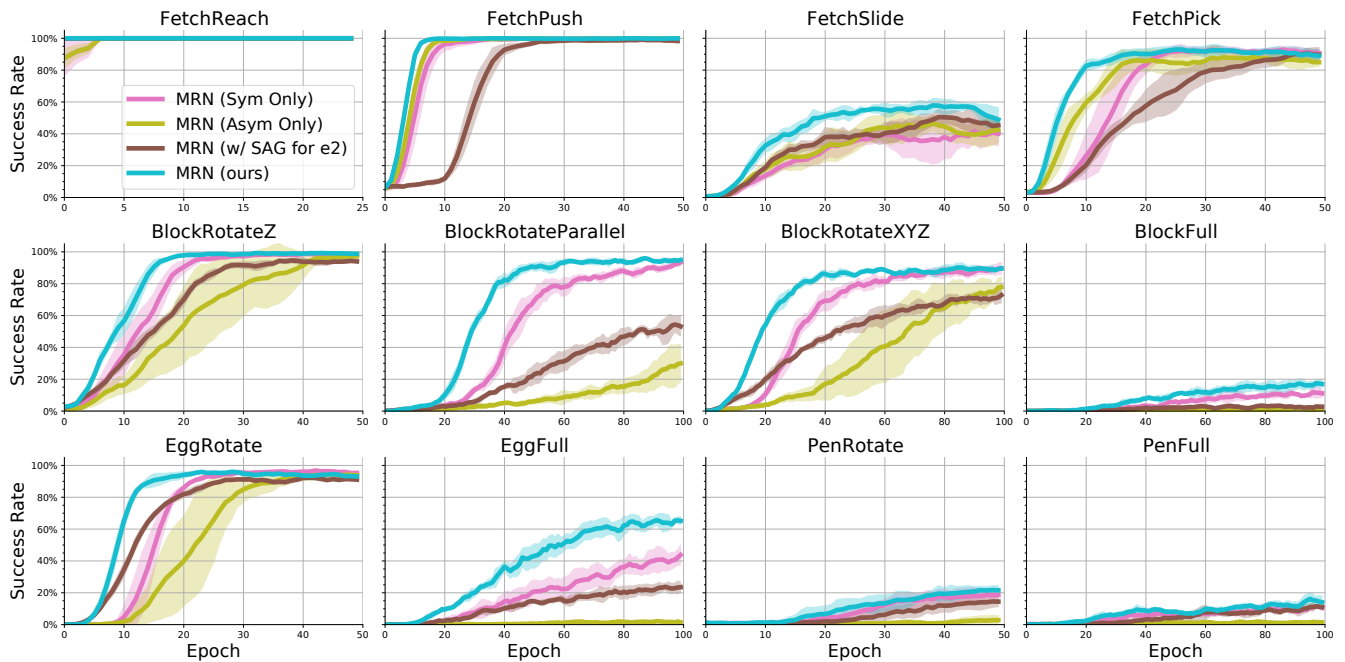


Figure 6: Ablation study on individual symmetric/asymmetric parts of MRN, and on feeding all  $(s, a, g)$  to  $e_2$ .

design, we check what happens when  $h_{sa} = e_1(s, a)$  but  $h_{sg} = e_2(s, a, g)$ . The result is in Fig. 6 (w/ SAG for  $e_2$ ). We observe that feeding all  $s, a, g$  as input to  $e_2$  confuses the network and prevents it from distinguishing between the roles of  $e_1$  and  $e_2$ .

## Conclusion

We present the simple yet theoretically-backed metric residual network (MRN) for GCRL. As large models are popular, exploring efficient inductive biases for network design is significant. Future research can extend MRN to general RL.

## Acknowledgements

The research was conducted in both the statistical learning and AI group (SLAI) led by Qiang Liu and the Learning Agents Research Group (LARG) led by Peter Stone in computer science at UT Austin. SLAI research is supported in part by CAREER-1846421, SenSE-2037267, EAGER-2041327, and Office of Navy Research, and NSF AI Institute for Foundations of Machine Learning (IFML). LARG research is supported in part by NSF (CPS-1739964, IIS-1724157, FAIN-2019844), ONR (N00014-18-2243), ARO (W911NF-19-2-0333), DARPA, GM, Bosch, and UT Austin's Good Systems grand challenge. Peter Stone serves as the Executive Director of Sony AI America and receives financial compensation for this work. The terms of this arrangement have been reviewed and approved by the University of Texas at Austin in accordance with its policy on objectivity in research. Special thanks to Xuchen Ma for the valuable discussion on goal-conditioned reinforcement learning.

## References

- Andrychowicz, M.; Wolski, F.; Ray, A.; Schneider, J.; Fong, R.; Welinder, P.; McGrew, B.; Tobin, J.; Pieter Abbeel, O.; and Zaremba, W. 2017. Hindsight experience replay. *Advances in neural information processing systems*, 30.
- Borsa, D.; Barreto, A.; Quan, J.; Mankowitz, D.; Munos, R.; Van Hasselt, H.; Silver, D.; and Schaul, T. 2018. Universal successor features approximators. *arXiv preprint arXiv:1812.07626*.
- Dayan, P. 1993. Improving generalization for temporal difference learning: The successor representation. *Neural computation*, 5(4): 613–624.
- Fujimoto, S.; Hoof, H.; and Meger, D. 2018. Addressing function approximation error in actor-critic methods. In *International conference on machine learning*, 1587–1596. PMLR.
- Haarnoja, T.; Zhou, A.; Hartikainen, K.; Tucker, G.; Ha, S.; Tan, J.; Kumar, V.; Zhu, H.; Gupta, A.; Abbeel, P.; et al. 2018. Soft actor-critic algorithms and applications. *arXiv preprint arXiv:1812.05905*.
- Hong, Z.-W.; Yang, G.; and Agrawal, P. 2022. Bilinear value networks. *arXiv preprint arXiv:2204.13695*.
- Kulkarni, T. D.; Saedi, A.; Gautam, S.; and Gershman, S. J. 2016. Deep successor reinforcement learning. *arXiv preprint arXiv:1606.02396*.
- Lillicrap, T. P.; Hunt, J. J.; Pritzel, A.; Heess, N.; Erez, T.; Tassa, Y.; Silver, D.; and Wierstra, D. 2015. Continuous control with deep reinforcement learning. *arXiv preprint arXiv:1509.02971*.
- Littman, M.; and Sutton, R. S. 2001. Predictive representations of state. *Advances in neural information processing systems*, 14.
- Mahadevan, S.; and Maggioni, M. 2005. Value function approximation with diffusion wavelets and laplacian eigenfunctions. *Advances in neural information processing systems*, 18.
- Pitis, S.; Chan, H.; Jamali, K.; and Ba, J. 2020. An inductive bias for distances: Neural nets that respect the triangle inequality. *arXiv preprint arXiv:2002.05825*.
- Plappert, M.; Andrychowicz, M.; Ray, A.; McGrew, B.; Baker, B.; Powell, G.; Schneider, J.; Tobin, J.; Chociej, M.; Welinder, P.; et al. 2018. Multi-goal reinforcement learning: Challenging robotics environments and request for research. *arXiv preprint arXiv:1802.09464*.
- Schaul, T.; Horgan, D.; Gregor, K.; and Silver, D. 2015. Universal value function approximators. In *International conference on machine learning*, 1312–1320. PMLR.
- Singh, S. P.; Littman, M. L.; Jong, N. K.; Pardoe, D.; and Stone, P. 2003. Learning predictive state representations. In *Proceedings of the 20th International Conference on Machine Learning (ICML-03)*, 712–719.
- Sutton, R. S.; and Barto, A. G. 2018. *Reinforcement learning: An introduction*. MIT press.
- Wang, T.; and Isola, P. 2022. On the Learning and Learnability of Quasimetrics. *arXiv preprint arXiv:2206.15478*.